Università degli Studi di Napoli Federico II

Scuola di Dottorato in Medicina Clinica e Sperimentale

Dipartimento di Scienze Odontostomatologiche e Maxillo-Facciali

DOTTORATO DI RICERCA IN:

SCIENZE ODONTOSTOMATOLOGICHE

XXII CICLO

TESI

"Different titanium surfaces influence in vitro the biological behavior of SaOS-2 human osteoblast-like cells"

Coordinatore **Candidato**

Prof. Sandro Rengo **Dott. Gabriele Capece**

Anni Accademici 2006-2009

INDEX

INTRODUCTION

The biological phenomena at the bone/implant interface leading to implant osseointegration depends on several factors, including implant macrostructural, microstructural and ultrastructural properties. In order to increase the bone/implant contact as well as optimize bone healing processes, each of these aspects has been thoroughly investigated in several studies [1-10].

More than macrostructural features, the superficial layer of titanium-oxide and the implant surface microstructure seem to deeply affect bone/fixture interactions [11-13].

After the initial contact with biological fluid, implant surface idratation occurs with absorption of ions, proteins, glycolipids, proteoglycans, polysaccharides, and a stable fibrin-platelet network is established. Cell migration, adhesion, proliferation, and differentiation with extra-cellular matrix (ECM) production and deposition at the implant surface are the most important following events.

Several studies [7, 8, 13-20] have shown that a rough surface, when compared to a relatively smooth one, grants better biomulecular absorption due to a wider surface, increases extra-cellular matrix production and promotes the differentiation of the mesenchymal cells toward an osteoblastic phenotype.

Mesenchymal cells may be able to detect variations of the superficial geometry through focal contact mechanisms, and therefore variate their own phenotypical expression: adhesion, causing a modification of the cellular shape, generates a signal that, transducted through the cytoskeleton to the nucleus, may produce a differentiation

towards an osteoblastic cellular typology [21-24]. Superficial roughness variation of only 1 μm may produce different cellular responses [25].

Different industrial treatments may modify the chemical features and thickness of the oxide layer as well as surface morphology and roughness. Optimal roughness and superficial morphology are still controversial and need to be clearly defined.

SaOS-2 is a mature osteoblastic cell line, derived from a human osteosarcoma, that several studies have demonstrated to be a relevant cell model, due to its large analogies with immature osteoblast cells [26-29] and better manageability when compared to primary human cell culture [30].

The aim of the present study was to evaluate *in vitro* the biological behavior of SaOS-2 cells, cultured on two different titanium surfaces, smooth and sandblasted-acid-etched, by investigating morphology, adhesion, including the expression of some integrins, proliferation, phenotypical bone expression and ECM deposition.

The behaviour of SaOS-2 cells on titanium surfaces *in vitro* may provide relevant information for the osseointegration process *in vivo*.

MATERIALS AND METHODS

Titanium Disks

Commercially pure titanium disks (2 cm in diameter and 2 mm in thickness) with two different surfaces (Sweden & Martina, Due Carrare, Italy) were used: a relatively smooth, machined surface (S) and a sandblasted-acid-etched surface (SBA). Titanium samples were subjected to a routine plasma cleaning in order to minimize surface contamination. The disks were then subjected to several steps of conventional solvent cleaning and placed in a cold-plasma reactor (Gambetti Kenologia, Milano, Italy). Furthermore, the disks were treated with air-plasma, at 100W and a flow rate of 20 scc/m (standard cubic cm/minute) for 15 min, rinsed with distilled water, and autoclaved prior to cell culture experiments.

Cell Culture

Human osteoblast-like SaOS-2 cells (ATCC85-HTB) were cultured in Dulbecco's modified Eagle's medium (DMEM) (Sigma, St. Louis, MO, USA), with 10% heat-inactivated fetal calf serum (FCS) (Gibco, Grand Island, NY, USA), 2 mM L-glutamine and 10 U/ml penicillin/streptomycin (Sigma, St. Louis, MO, USA) in a humidified 95% air/5% CO_2 incubator, at 37°C. The medium was changed every 3-4 days. Cells were detached by 0.5 mmol/L ethylendiammintetraacetate in calcium and magnesium-free phosphate-buffered saline (PBS) with 0.05 % trypsin. For all experiments, $1.5x10^6$ cells were plated and cultured on titanium disks in 60 mm-culture plates (Sarstedt, Newton,

NC, USA). Cells grown on a polyester plastic surface were used as a control. All experiments were carried out in quadruplicate and repeated three times.

Scanning Electron Microscopy (SEM)

Titanium disk surfaces were analysed by scanning electron microscopy (SEM).

The disks did not require any special preparation for SEM examination and no significant difference was evident after the treatment with autoclave. Initially, an experiment was designed to evaluate cell morphology and times of cell subconfluence and confluence on both titanium disks. SaOS-2 cells were cultured on titanium disks up to 96 h. Culture for SEM analysis was performed in triplicate. The medium was removed from the wells and the disks were slowly washed with PBS and fixed at selected time points, first with 1% glutaraldehyde in 0.1M buffer phosphate at pH 7.3 for 1 h, and a second time with 1% osmium tetraoxide in 0.1 M buffer cacodylate at pH 7.4 for 1 h. The disks were washed with PBS three times, dehydrated in a graded series of ethanol (30%, 50%, 70% and 90%) and placed in a 100% ethanol bath and rinsed three times (30 min. x 3). The disks were critical-point dried, then mounted on copper stubs which were introduced into a sputter coater and coated with gold. The surfaces were then observed using the scanning electron microscope (JSM-6700F, JEOL Ltd., Japan) at an accelerating voltage of 100 kV.

^{3}H-thymidine Incorporation and Cell Proliferation Assay

To determine the proliferation of SaOS-2 cells on titanium surfaces, we measured

^{3}H-thymidine incorporation. SaOS-2 cells were plated on titanium disks and cultured up to 14 days in the presence of 100 μCi of ^{3}H-thymidine. Cells were harvested, counted in a Neubauer cytometer at given times (24, 72, 96 hrs; 7th and 14th day), and absorbed onto nitrocellulose paper; radioactivity was then counted in a β-counter (Beckman LS1801, Milano, Italy). Results were expressed as mean incorporation at the experimental point (counts *per* min)/10^{4} cells. Titanium disks without cells and medium alone were used as negative controls.

Cell Attachment Assay

SaOS-2 cells were grown on 60 mm plastic culture dishes (Sarstedt, Newton, NC, USA) until 50% confluence. Cells cultured for 2 days in the presence of ^{3}H-Thymidine 10 μCi/ml were harvested and ^{3}H-Thymidine labeled cells were counted with a β-counter (Beckman LS 5000, CA, USA). Cells were plated on the titanium disks and incubated for 3 hrs at 37°C, 5%CO_2. Disks were washed with PBS, transferred into counting tubes with liquid scintillation (Wallac, Milton Keynes, UK) and the radioactivity was measured as above.

Alkaline Phosphatase and Interleukine-6 measurement

Alkaline phosphatase (ALP) was determined with p-nitrophenylphosphate as a substrate. SaOS-2 cells, plated on titanium disks, were analysed at the same time intervals as described above. Cells were scraped into a 500-μl ice-cold harvest buffer (10mM Tris HCI, pH 7,4, 0,2% NP-40 and 2mM phenylmethylsulfonyl fluoride, PMSF). Enzymatic

activity was measured by an automatic analyser (Hitachi 747, Boheringer Mannheim, Indianapolis, IN, USA). The results were expressed as UI/(enzyme activity)/10^4 cells.

A quantitative analysis to determine the production of Interleukine-6 (IL-6) was performed by Enzyme-linked Immunoassay (ELISA) (Quantikine, R&D Systems, Minneapolis, MI, USA). SaOS-2 cells were plated on titanium disks at 24, 72, 96 hrs and 7^{th}, 14^{th} days of culture. The results were expressed as IL-6 concentration (pg/mL) /10^4 cells.

ECM Deposition: in situ Enzyme-linked Immunoassay

A quantitative analysis of some ECM components (CoI, FN and TN) produced by SaOS-2 cells, cultured on titanium disks up to 14 days, was performed by in situ Enzyme-linked Immunoassay. SaOS-2 cells were plated on titanium surfaces and cultured for up to 14 days. At the same time intervals as above, cells were fixed on titanium surfaces by 50% (vol/vol) methanol-acetone for 10 min at room temperature and air-dried. Disks were incubated with calcium and magnesium-free phosphate-buffered saline (PBS)/0.5 % bovine serum albumin (BSA), for 2 hrs at 4°C, then filled with 50 µL of one of the following rabbit anti-sera: anti-collagen I (Co I), anti-fibronectin (FN) or anti-tenascin (TN) (Chemicon, Temencula, CA, USA), in PBS/0.5 % BSA and 0.2 % Tween 20, and allowed to react for 1 hr at room temperature. Plates were then washed with PBS, filled with 50 µL horseradish peroxidase-conjugated anti-rabbit IgG in PBS, 0.2% Tween 20, allowed to react for 1 hr, washed again with PBS and filled with 150 µL of 1 mg/mL o-phenyl-enediamine, 0.006% hydrogen peroxide, 0.1 M citrate buffer, pH 5.0. After 30 min of incubation, the absorbance at 450 nm was

measured by a spectrophotometer. Titanium disks without cells and disks coated with purified ECM components were used as controls. To evaluate the effect of serum on ECM deposition of SaOS-2 cells, serum-starved cells, cultured in DMEM 0.5% BSA, were used as controls.

Fibronectin and Tenascin Deposition by Western Blotting

The expression of fibronectin and tenascin by SaOS-2 cells was also investigated by Western blotting. Cell lysates were collected by scraping on titanium disks and centrifuged at 14.000 rpm for 5 min at 4°C. Supernatants were harvested and protein concentration in cell lysates was determined by a colorimetric assay (BioRad, Richmond, CO, USA). For each sample, 100 μg of total proteins was incubated 5 min at 90°C in Laemmli sample buffer and separated by electrophoresis in 10% SDS-polyacrylamide gels. Gels were electroblotted on PVDF filters (Millipore, Bedford, MA, USA); membranes were blocked with 5% fat-free dry milk, 1% ovalbumin, 5% fetal calf serum (FCS) and 7.5% glycine for 30 min at room temperature. After three washes in washing solution (PBS/0.1% ovalbumin, 0.1% fat-free dry milk, 1% FCS), membranes were incubated overnight at 4° C with the specific primary monoclonal antibodies: anti-FN (Chemicon, Temencula, CA, USA) and anti-TN (Sigma, St. Louis, MO, USA). After four 5 min washes, at room temperature, with washing solution, membranes were incubated for 30 min at room temperature with horseradish peroxidase-conjugated secondary antibody (BioRad, Richmond, CO, USA), diluted to 1:3000 in PBS. After three washes in washing solution and three final washes in T-TBS (50mM Tris, pH 7.5;

0.5M NaCl; 0.2% Tween 20), membranes were stained with an enhanced chemoluminescence (ECL) detection kit (Amersham, Little Chalfont, UK).

A quantitative analysis was performed by Scanner Densitometry (Agfa Snapscan 1212, Agfa-Gevaert, Mortsel, BE).

Reverse Transcriptase - Polimerase Chain Reaction (RT-PCR)

Total RNA was isolated from cells cultured at 8 days using a total RNA isolation reagent (Trizol Reagent, Invitrogen, Paisley, UK), according to the manufacturer's instructions. Contaminating DNA was digested with DNase using a DNase Kit (Trizol Reagent, Invitrogen, Paisley, UK) and 2µg of total RNA was reverse transcribed with 100 U of a DNA polymerase (Super Script II RNAse H-Reverse Transcriptase, Invitrogen, Paisley, UK) in a volume of 40µl, using 100 mM random hexamer primers (Roche, Indianapolis, IN, USA) according to the manufacturer's instructions. Primer sequences for RT-PCR were as follows:

Collagen type I forward primer, 5'-GAG GAA GGC CAA GTC GAG G-3';

Collagen type I reverse primer, 5'-CCG AGT GAA GAT CCC CTT TTT A-3'; and generated an 86 base-pair fragment.

The amplification was established using a DNA Thermal Cycler (Perkin Elmer Cetus, Norwalk, CT, USA) for 35 cycles as follows: denaturation: 95°C for 45s; annealing: 60° C for 30s; extension: 72°C for 30s.

At the beginning of the reaction, a cycle at 95°C for 5 min was carried out to activate Taq Polimerase.

Real-time quantitative PCR

A quantitative assay for type I (alpha 1) collagen mRNA expression was established using a Real-time PCR system (ABI Prism 7000 Sequence Detection System, Applied Biosystems, Foster City, CA, USA). All measurements were normalized to an endogenous control using the 101 bp fragment at 3' of the beta-glucuronidase region. PCR oligo-primers were: h-COL1A1 forward primer 5'-GAG GAA GGC CAA GTC GAG G-3' and h-COL1A1 reverse primer 5'-ACG TCT CGG TCA TGG TAC CTG-3' generating an 86 bp fragment; h-GUSB forward primer 5'-GAA AAT ATG TGG TTG GAG AGC TCA TT-3' and h-GUSB reverse primer 5'-CCG AGT GAA GAT CCC CTT TTT A-3'.Real-time PCR was performed using a Real-rime PCR solution (SYBR Green PCR Master Mix 2X, Applied Biosystems, Foster City, CA, USA) and 50 ng of cDNA in a total volume of 15µl. Each sample was run in triplicate, for both type I (alpha 1) collagen and beta glucuronidase. The PCR cycling profile consisted of AmpErase UNG incubation for 2 min at 50°C and AmpliTaq Gold activation for 10 min at 95°C, as predenaturation steps, and in 50 two-step cycles at 95°C for 15 s, and at 60°C for 60 s. For type I (alpha 1) collagen mRNA relative quantification, the comparative Ct method was used according to the manufacturer's instructions (Applied Biosystems, Foster City, CA, USA).

Integrin subunits expression: Flow Cytometric Analysis

SaOS-2 cells plated on titanium surfaces and cultured up to 96 hrs were harvested by treatment with trypsin/PBS and incubated with specific monoclonal antibodies against integrin subunits, i.e. anti-α2 (kindly donated by Dr. A.E.G.Kr. Von Dem Borne,

Amsterdam, Netherlands), anti-α (Telios, San Diego, CA, USA 5), anti-α6 (kindly donated by Dr. M.E. Hemler, Boston, MA, USA) and anti-β1(Telios, San Diego, CA, USA), for 1 hr at 4°C, in 0.5% BSA in PBS. Cells were then washed in the same buffer and incubated with the second fluorescein-conjugated antibody for 30 min at 4°C. Finally, cells were suspended in BSA/PBS and analysed by flow cytometry (FACScan, Beckton Dickinson, Mountain View, CA, USA). Non specific IgGs of the same isotype were used as a negative control. Results were reported as fold of expression, as compared to the negative control.

Statistical Analysis

The data obtained in the present study were calculated as mean +/- S.D. Statistical analysis for normally distributed parametric data was performed using the Student's t-test, and the differences were considered statistically significant with "p" values less than 0.05. For non parametric data obtained by Real-time analysis, the differences were analysed using the REST program and the Pair Wise Fixed Reallocation Randomisation test. Randomisation tests with a pair-wise reallocation are considered the most appropriate approach for this application. They are more flexible than non-parametric tests based on ranks (Mann-Whitney, Kruskal-Wallis) and do not suffer a reduction in power relative to parametric tests (t-test, ANOVA). A p-value <0.05 was considered significant.

RESULTS

Cell Morphology

Titanium surfaces of Smooth (S) and Sandblasted-acid-etched (SBA) disks were observed by Scanning Electron Microscopy (SEM) at 600X magnification. As shown in Figure 1A, the surfaces of S disks without cells after the treatment with autoclave were very smooth. On the contrary, the surfaces of the SBA disks were characterized by pits and bumps; furthermore, grain boundaries were infrequently observed (Figure 1B). SaOS-2 cells plated on titanium surfaces were examined after 96h by SEM and differences in cellular morphology on both surfaces were observed. Cells grown on the S titanium surface tended to grow in a flat and spread monolayer with a parallel orientation (Figure 1C). Cells grown on the SBA titanium surface tended to orient themselves according to surface discontinuity, showing clusters of multilayered cells. Cell shape was also irregular, presenting numerous cellular extensions and more extended processes (Figure 1D).

Cell Proliferation

For both surfaces, the number of cells increased gradually during the culture period, proliferation peaking on the last day of culture (14 days).

Cell proliferation was not influenced by the type of surface, as shown in Figure 2. The observed differences in the growth curves of the two different surfaces were not statistically significant ($p>0.05$).

Production of Bone Differentiation Markers

To evaluate cellular differentiation, we analysed the production of two osteoblastic markers involved in the mineralization process: Alkaline Phosphatase (ALP) and Interleukine-6 (IL-6). The results (Figure 3A) demonstrated a significant increase in ALP activity on both surfaces after 14 days of culture ($p<0.05$), but there was no statistically significant difference between the evaluated surfaces ($p>0.05$).

Also IL-6 production increased significantly after 14 days (Figure 3B) with an earlier and more gradual trend when compared to ALP production. Once again, there was no statistically significant difference between the two titanium surfaces ($p>0.05$).

Production of Extracellular Matrix (ECM)

To investigate ECM production, we estimated the total amount of Fibronectin (FN), Tenascin (TN) and Collagen I (Co I) synthesized by SaOS-2 cells by ELISA in situ (Figure 4, panels A, B and C, respectively). The difference between S and SBA surfaces was not significant for FN and TN deposition (panel A and B); on the contrary, the Co I production was significantly higher in SaOS-2 cells cultured on SBA titanium surfaces as compared to S surfaces, starting from day 7 (panel C) ($p<0.05$). Serum-starved cells, cultured in DMEM/0.5% BSA, still produced ECM components, although to a lower extent, thus showing that matrix production was not due to the deposition of serum components (data not shown). Production of FN and TN was confirmed by Western blotting analysis of SaOS-2 cell lysates after incubation overnight at 4° C with the specific primary monoclonal antibodies that showed bands, of variable intensities, with

the expected molecular weights of 220 kDa for FN and 200 kDa for TN. A quantitative analysis was also performed; again no statistically significant difference in the expression of FN (Figure 5A) and TN (Figure 5B) was observed between the two surfaces. Due to high molecular weight of Co I, Western blotting analysis for this protein was not performed.

RT-PCR and Real-time quantitative PCR

Type I collagen deposition was also investigated by RT-PCR and Real-time quantitative PCR. The results show that the expression of type I collagen mRNA is 2-fold higher ($p<0.05$) in SaOS-2 cells cultured on SBA titanium surfaces as compared to S surfaces (Figure 6), in agreement with the data obtained by enzyme-linked immunoassay in situ.

Cell Attachment Assay

In order to evaluate whether the increase in matrix deposition had a functional correspondence, we first analysed how cell attachment was affected by different titanium surfaces. SaOS-2 cells were labelled with ^{3}H-Thymidine, plated on titanium disks and allowed to attach for 3 h. The radioactivity retained by the disks after extensive wash was 8780 +/- 864 and 6800 +/- 728 (mean c.p.m. ± SD) for S and SBA disks respectively. Differences were not statistically significant ($p>0,05$), demonstrating that the attachment of SaOS-2 cells was only slightly affected by the different titanium surfaces.

Expression of Integrin Subunits

We then evaluated the expression of the receptors involved in the adhesion of SaOS-2 cells to titanium surfaces. In particular, we analysed expression of α2, α5, α6 and β1 integrin subunits in SaOS-2 cells cultured up to 96 hrs by flow cytometry (Figure 7, panels A and B). All integrin subunits increased between 24 and 96 hrs of culture on the two different surfaces (panel A). The expression of all integrin subunits was higher in SBA surfaces as compared to S surfaces (panel B), even though a significant difference was observed only for the α2 subunit (SBA vs S $p<0.05$).

DISCUSSION

Dental implant osseointegration is a complex phenomenon depending on several factors and characterized by a long sequence of events [31-41].

Several studies suggest that surface properties of titanium implants are able to affect bone formation in different steps [8, 13, 14, 41-43].

Different industrial treatments may modify implant surface properties though optimal surface roughness and topography are still controversial.

Numerous studies [7, 8, 13-20, 42, 44] have shown that a rough surface, when compared to a smooth one, grants a better biomolecular adsorption, increases extracellular matrix production and promotes the differentiation of the pluripotent mesenchymal cells toward an osteoblastic phenotype.

After the initial phase of implant surface idratation with biological fluids and molecular absorption, a stable fibrin-platelet network is established.

Fibrinogen absorption, platelet adhesion, and aggregation are greater on a micro-roughened surface when compared to a machined surface [45]. Morphological surface properties may have a critical role in fibrin retention, both increasing available surface and providing appropriate attachment sites.

After molecular absorption, the most important subsequent events are the migration of pluripotent undifferentiated cells from perivascular connective tissue and their adhesion to the implant surface, followed by osteoblastic differentiation and proliferation [39-41].

Specific membrane receptors, the integrins, allow mesenchymal cells and osteoblasts to bind to ECM and/or plasma adhesion proteins [46] adsorbed by the implant surface. Fibronectin and tenascin represent the main ligands of integrins.

Surface texture seems to affect the expression of fibronectin and tenascin integrins, to modify their aggregation, and determine changes in cellular shape, proliferation and differentiation [47].

The rationale of the influence of surface texture should be recognized by the ability of mesenchymal cells to detect the variations in surface geometry through the mechanisms of focal contact and, therefore, varying its phenotypic expression: the adhesion may lead, by means of a change of the cellular shape, to transduce a signal through the cytoskeleton to the nucleus that induces a differentiation toward the osteoblastic phenotype [22-24, 35].

Optimal roughness should be in the range of cellular dimension. The mean length of a mesenchymal cell varies from about 5 to 12 microns, so a surface microtopography with a dimensional range greater than the cell length may be read as smooth [48]. Zinger et al. [49] observed that osteoblasts tend to aggregate in 100 micron wide craters artificially produced on titanium surfaces: these craters show structural features similar to the cavities produced by osteoclastic resorption, the surface that osteoblasts prefer *in vivo* to synthetize osteoid.

Probably the use of microtopographies, detected by cells as rough, stimulates an increased expression of osteoblastic phenotype, potentially leading to an improved production of bone [41].

The ability of osteogenic cells to differentiate into functional osteoblasts is influenced, in addition to factors related to implant surface morphology, by other aspects such as local oxygen tension, nutrient availability, the presence of local and systemic regulatory factors.

In our study we investigated *in vitro* morphology, adhesion, proliferation and differentiation of human osteoblast-like cells SaOS-2 on two different titanium surfaces, smooth and sandblasted-acid-etched.

SaOS-2 is a mature cell line derived from a human osteosarcoma, which several studies [26-29] demonstrate to be a relevant cell model, due to is large analogies with immature osteoblastic cells. Several primary and transformed cell lines have been used to develop culture systems to study the interaction of cells with implant biomaterials [7, 16-18, 20, 26-30, 50-55].

Shapira and Halabi [30] recently reported that, in contrast to primary cultured human osteoblasts that not always exhibit predictable results due to the tendency to lose the phenotype during cell culture steps, immortalized SaOS-2 cells show more manageability without loss of phenotypic expression. SaOS-2 cells also exhibit a more mature expression of osteoblastic phenotype when compared to other immortalized cell lines, representing a good *in vitro* model for the study of osseointegration.

At SEM analysis, SaOS-2 cells cultured on the two different titanium surfaces appeared flattened on both surfaces, even with more irregular shape on SBA surfaces suggesting a more complex and mature organization.

Literature data [26, 43] suggest that differentiation toward an osteoblastic phenotype correlates with a decrease in cell proliferation and an increase in production of the alkaline phospatase (ALP), a fundamental osteogenic activity marker [27, 56] .

Cell proliferation increased significantly up to 7 days of culture on both surfaces, according to the observations of Martin et al. [7], with no significative differences between the two surfaces ($p>0.05$).

With regard to alkaline phospatase production, the data showed a significant increase in ALP production on both surfaces, after 14 days of culture, with no significative differences between the two surfaces ($p>0.05$).

Therefore, the data of low proliferation and high ALP activity suggest that SaOS-2 cells on both surfaces express properties of differentiated osteoblasts.

Also the production of IL-6, the other bone differentiation marker examined, increased significantly after 14 days, but there was no statistically significant difference between the two titanium surfaces ($p>0.05$).

These results seems to indicate a marked tendency of the SaOS-2 cells cultured on both surfaces to differentiate towards an osteoblastic phenotype, although there aren't any significative differences between the examined surfaces.

The osteoblastic phenotypye differentiation was confirmed by the study of matrix deposition.

Collagen I (Co I), Fibronectin (FN) and Tenascin (TN) are among the components of the ECM produced by osteoblasts during cell differentiation [35], and represent the largest protein class of animal extracellular structures [57].

Collagen I, the major component of bone tissue, represents 90% of the whole body collagen [35] and represents the main structural protein of extracellular matrix [57].

Fibronectin and Tenascin represent two important matrix adhesion proteins that allow the crosslink between Co I, proteoglycans and ialuronic acid and the connection of this network to cytoskeletal microfilaments by means of transmembrane receptors [58-60].

The analysis of ECM production in SaOS-2 cultures showed that the synthesis of FN and TN increases over time on sandblasted/acid-etched surfaces but without remarkable differences when compared to control disks with smooth topography.

A statistically significant difference ($p<0.05$) between S and SBA surfaces was observed in CoI production at 7 days and 14 days of culture.

Data seem to indicate a higher level of extracellular matrix structural organization and therefore a more mature differentiation of osteoblast-like cells when cultured on a rough surface.

To investigate whether the increase in matrix deposition had a functional correspondence, we analysed cellular adhesion and the expression of the integrin receptors for Co I, FN and TN.

Cellular adhesion on the two different surfaces, in agreement with the observations of other studies, didn't show statistically significant differences ($p>0.05$) between the test surfaces [61].

The specific integrins for the three ECM components studied (Co I, FN and TN) are α2, α5, α6, respectively. We found an increased expression of these receptors on both surfaces, although a significant difference ($p<0.05$) between the two surfaces was

observed only for the α2 subunit. This observation strongly correlates with data on ECM production, since α2 recognizes CoI, the major ECM component.

Comparing these observations with our previous experimental studies [17, 18, 27, 44] which showed a more significative difference in the induction of ECM synthesis and organization relating to surface roughness, we can suppose that the treatment of sandblasting and acid-etching on tested titanium disks produces a surface that less, or more slowly, stimulates the SaOS-2 cells to produce extracellular matrix. The different synthesis and organization of ECM proteins might relate to the specific microtopography of the experimental titanium surface which may be read by osteoblastic-like cells as a smooth surface instead of a rough one with consequent changes in the cellular expression.

CONCLUSIONS

Preliminary data show that surface microtopography affects *in vitro* proliferation and differentiation of osteoblast-like cells, suggesting that implant surface properties may modulate *in vivo* the biological behaviour of osteoblasts in periimplant tissue healing.

Unlike other surfaces that we previously discussed, the sandblasted and acid-etched one with specific microstructure seems to induce, during the examined period, a less or slower response in SaOS-2 cells. Further studies are needed to support this evidence.

FIGURES

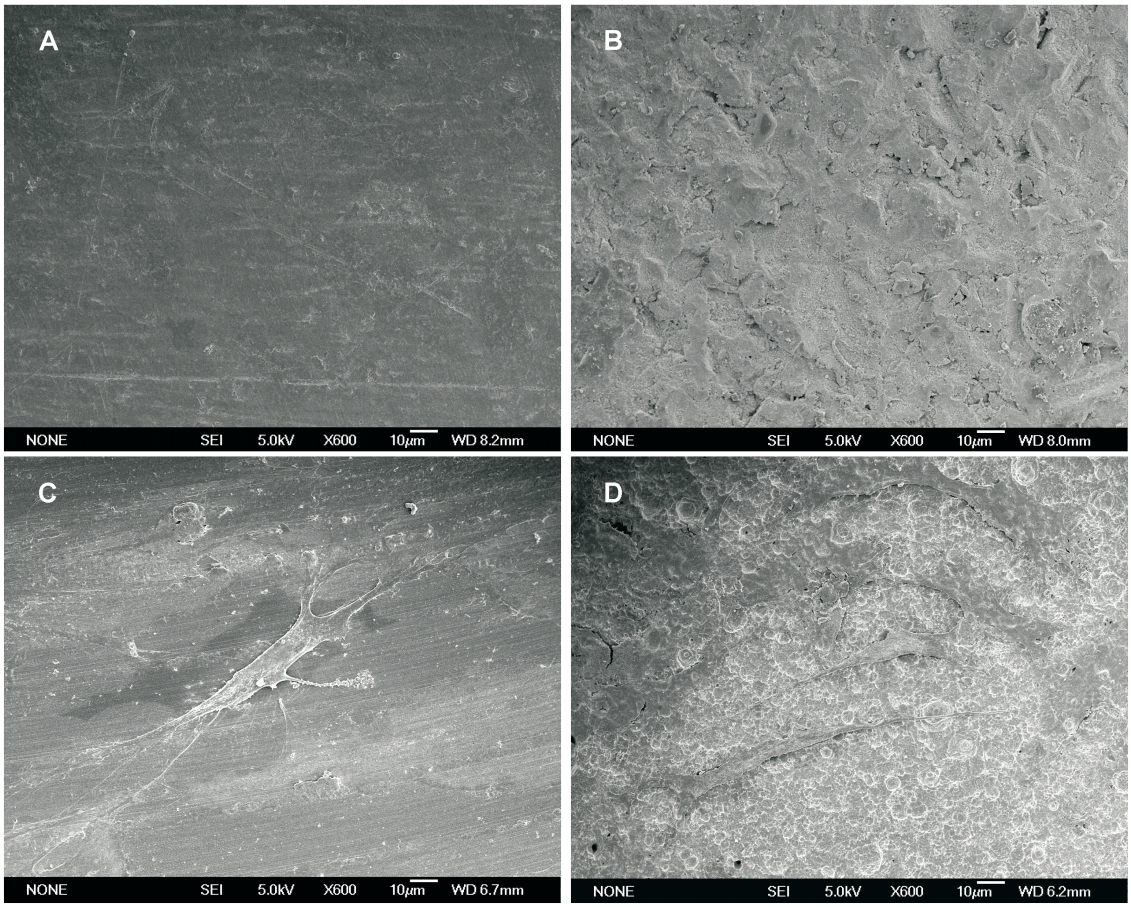

Figure 1

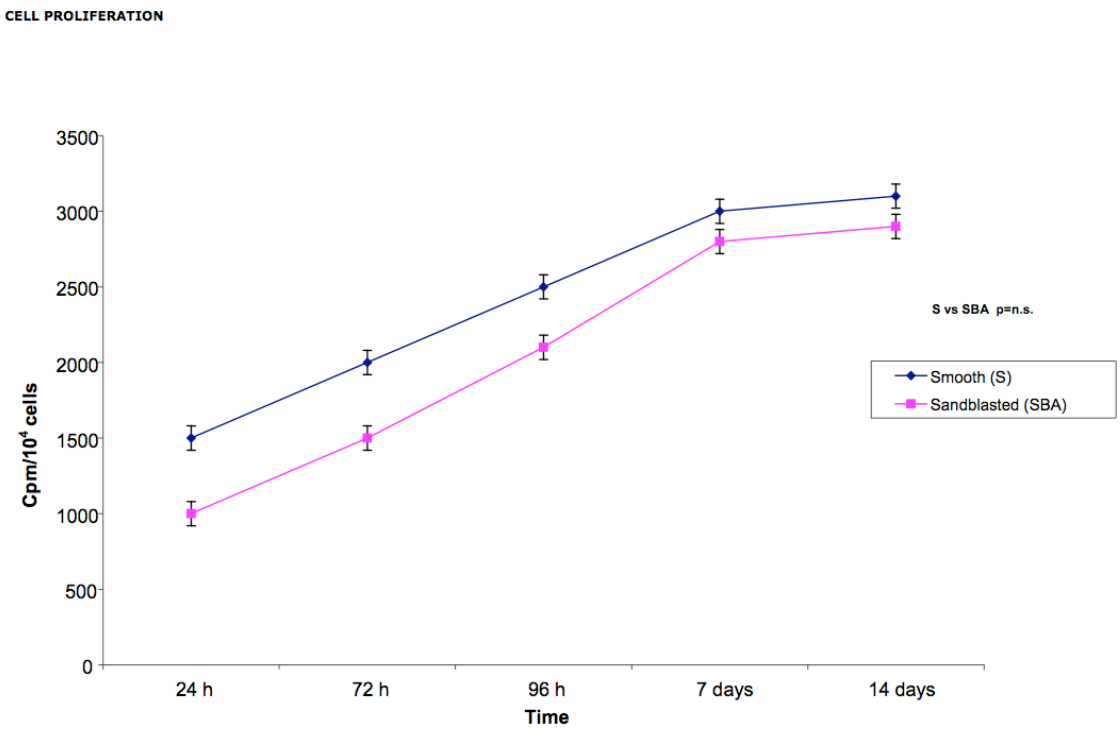
CELL PROLIFERATION
3500
3000
2500
2000
1500
1000
500
0
Cpm/10^4 cells
24 h
72 h
96 h
7 days
14 days
Time
S vs SBA p=n.s.
Smooth (S)
Sandblasted (SBA)

Figure 2

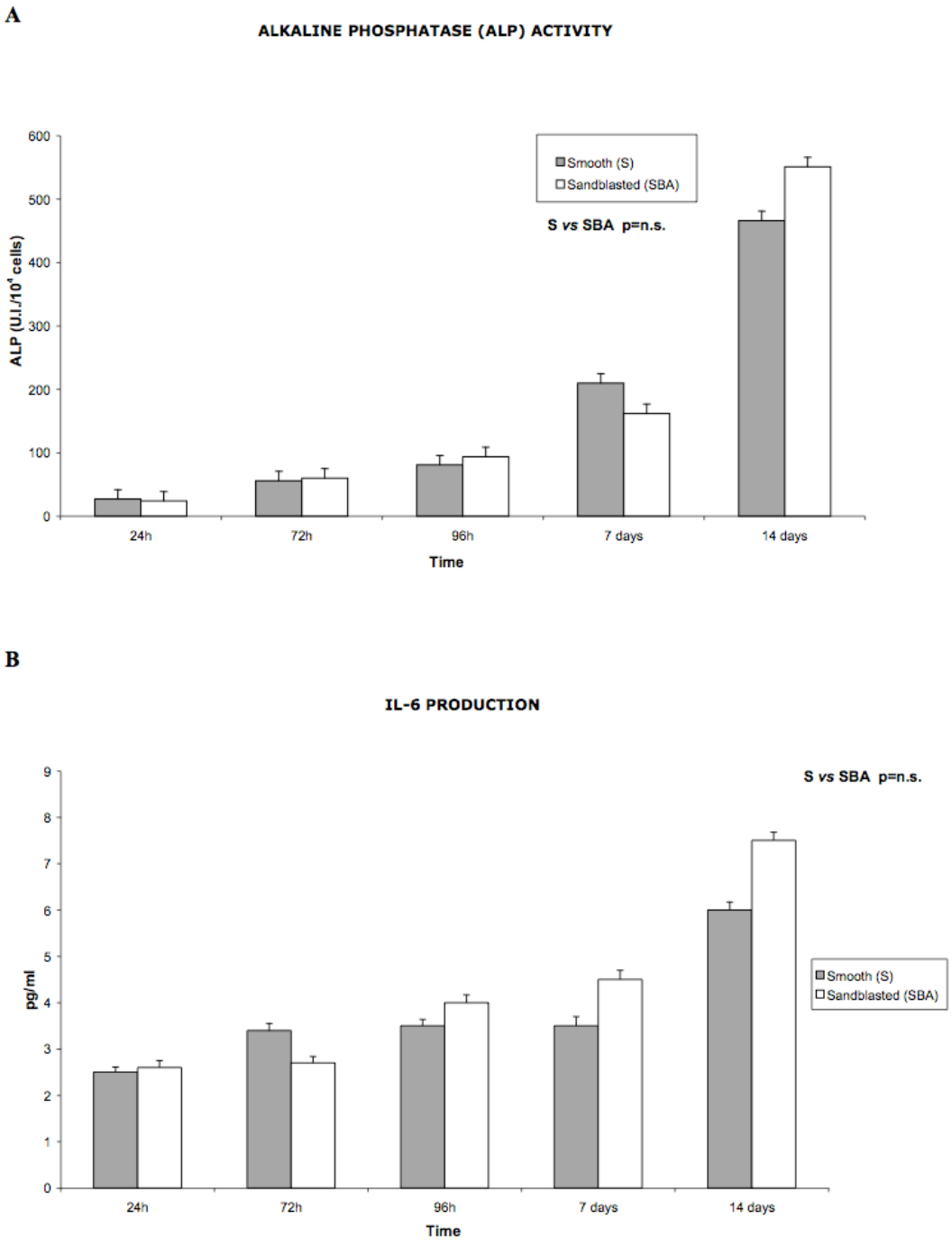
A
ALKALINE PHOSPHATASE (ALP) ACTIVITY
ALP (U.I./10⁴ cells)
600
500
400
300
200
100
0
Smooth (S)
Sandblasted (SBA)
S vs SBA p=n.s.
24h
72h
96h
7 days
14 days
Time
B
IL-6 PRODUCTION
pg/ml
9
8
7
6
5
4
3
2
1
0
S vs SBA p=n.s.
Smooth (S)
Sandblasted (SBA)
24h
72h
96h
7 days
14 days
Time

Figure 3

A

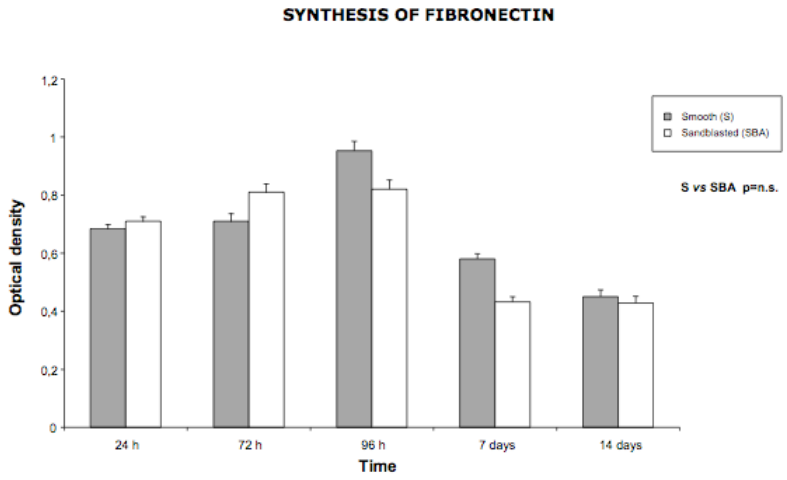
SYNTHESIS OF FIBRONECTIN
Optical density
1,2
1
0,8
0,6
0,4
0,2
0
24 h
72 h
96 h
7 days
14 days
Time
Smooth (S)
Sandblasted (SBA)
S vs SBA p=n.s.

B

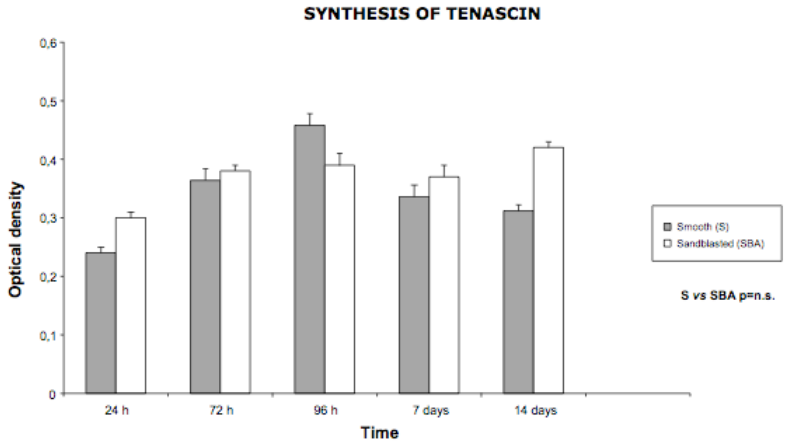
SYNTHESIS OF TENASCIN
Optical density
0,6
0,5
0,4
0,3
0,2
0,1
0
24 h
72 h
96 h
7 days
14 days
Time
Smooth (S)
Sandblasted (SBA)
S vs SBA p=n.s.

C

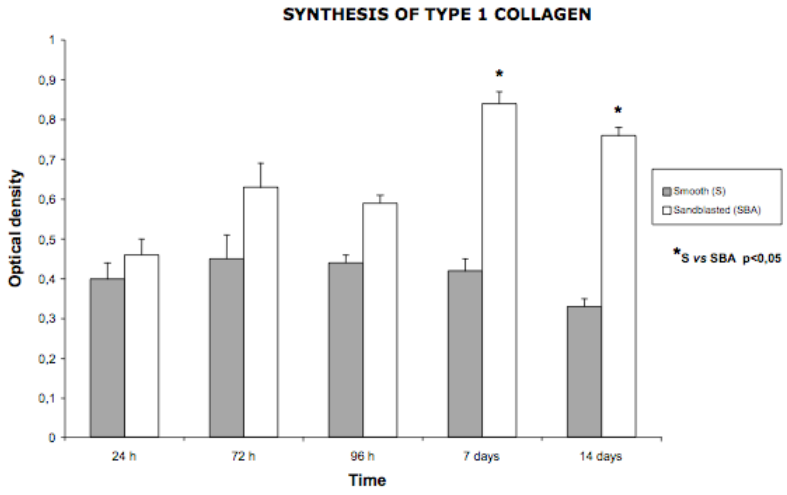
SYNTHESIS OF TYPE 1 COLLAGEN
Optical density
1
0,9
0,8
0,7
0,6
0,5
0,4
0,3
0,2
0,1
0
*
*
24 h
72 h
96 h
7 days
14 days
Time
Smooth (S)
Sandblasted (SBA)
*S vs SBA p<0,05

Figure 4

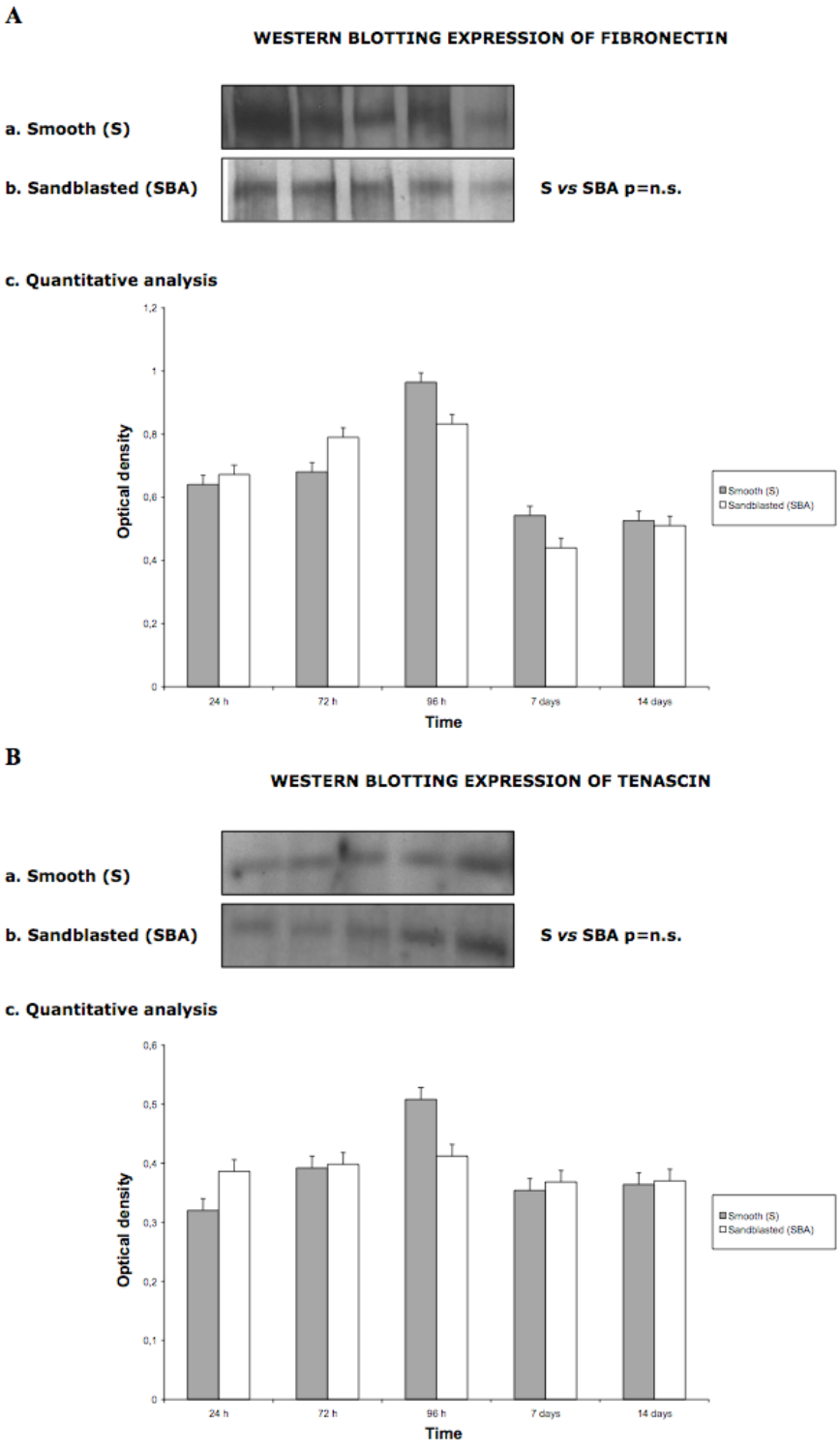
A
WESTERN BLOTTING EXPRESSION OF FIBRONECTIN
a. Smooth (S)
b. Sandblasted (SBA)
S vs SBA p=n.s.
c. Quantitative analysis
Optical density
1,2
1
0,8
0,6
0,4
0,2
0
24 h
72 h
96 h
7 days
14 days
Time
Smooth (S)
Sandblasted (SBA)
B
WESTERN BLOTTING EXPRESSION OF TENASCIN
a. Smooth (S)
b. Sandblasted (SBA)
S vs SBA p=n.s.
c. Quantitative analysis
Optical density
0,6
0,5
0,4
0,3
0,2
0,1
0
24 h
72 h
96 h
7 days
14 days
Time
Smooth (S)
Sandblasted (SBA)

Figure 5

A

TYPE 1 COLLAGEN MRNA EXPRESSION: RT-PCR

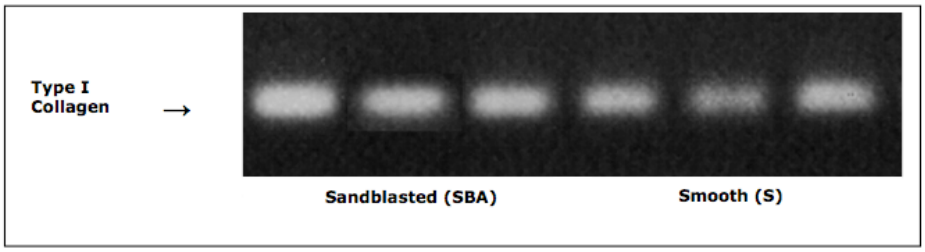

B

TYPE 1 COLLAGEN MRNA EXPRESSION: REAL-TIME PCR

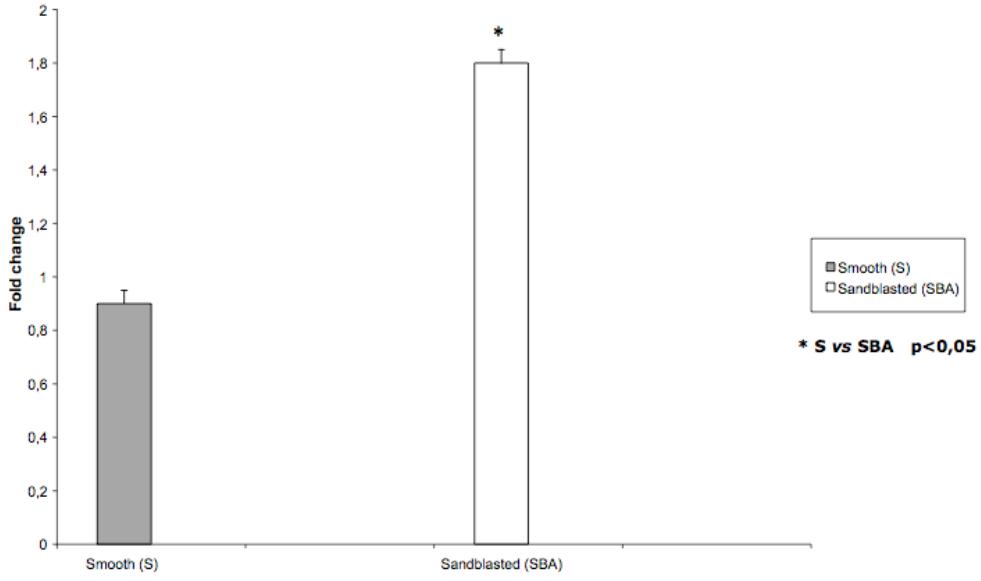

Figure 6

A

INTEGRIN EXPRESSION: FLOW CYTOMETRIC ANALYSIS

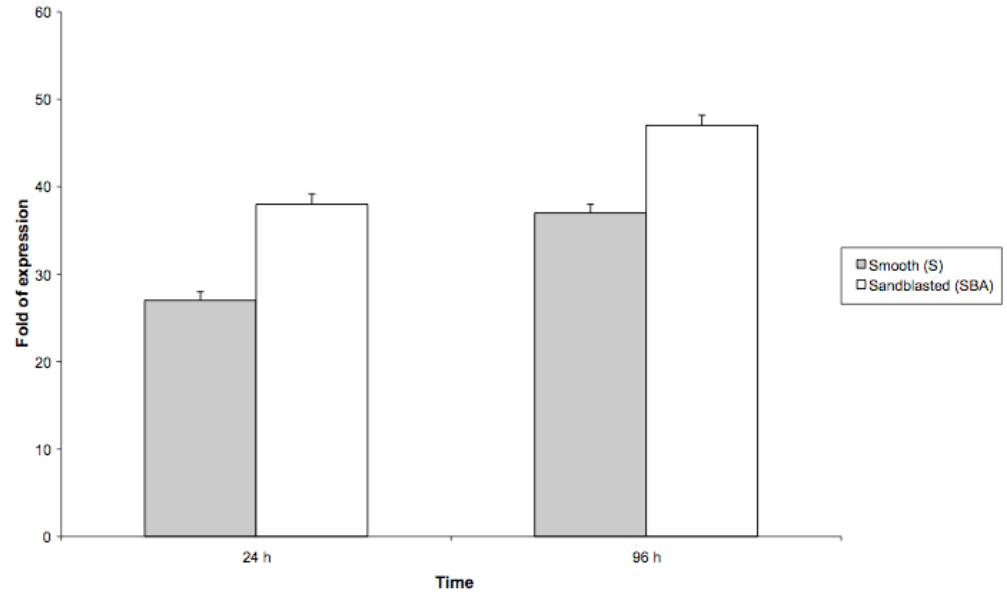

B

INTEGRIN SUBUNITS EXPRESSION: FLOW CYTOMETRIC ANALYSIS

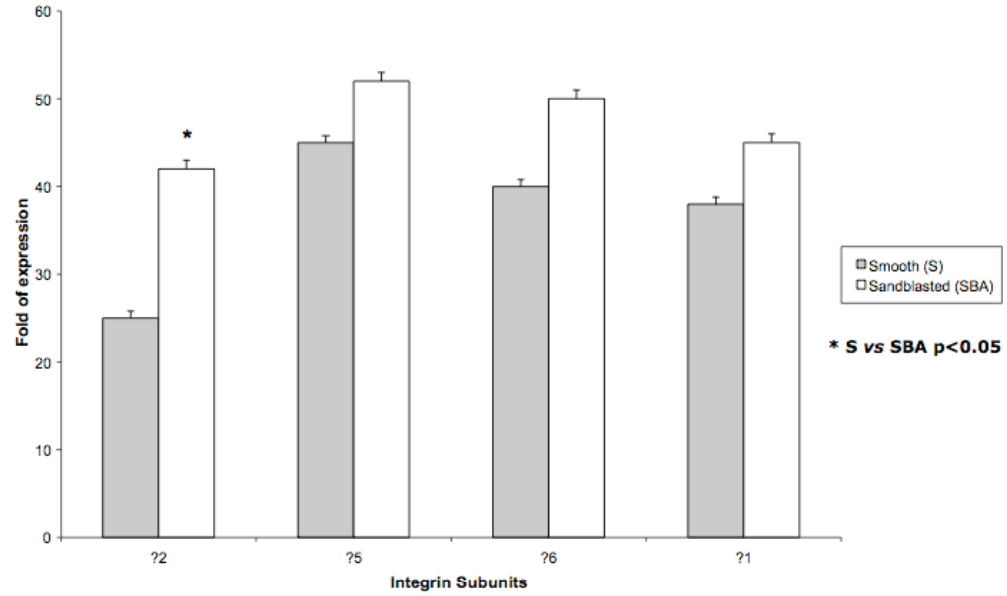

Figure 7

FIGURE LEGENDS

Figure 1. Scanning electron micrographs of disks' surfaces without cells after the autoclave treatment (A: Smooth surface; B: Sandblasted-acid-etched surface). Scanning electron micrographs of cultured SaOS-2 cells adhering to different titanium surfaces (C: Smooth surface; D: Sandblasted-acid-etched surface). (Magnification, 600X).

Figure 2. Cell proliferation curves of SaOS-2 cells on titanium surfaces. S vs SBA p=n.s. (not significant).

Figure 3. A) Alkaline phosphatase (ALP) activity of SaOS-2 cells on titanium surfaces determined by spectrophotometric analysis. S vs SBA p=n.s. (not significant). B) IL-6 production in SaOS-2 cells on titanium surfaces determined by enzyme-linked immunoassay in situ. S vs SBA p=n.s. (not significant).

Figure 4. Synthesis of extracellular matrix (ECM) proteins (FN, TN and Co I) in SaOS-2 cells on titanium surfaces determined by enzyme-linked immunoassay in situ. A) FN and B) TN deposition: S vs SBA p=n.s. (not significant); C) Co I deposition is significantly higher in SBA vs S $p<0.05$.

Figure 5. A) Western blotting expression of fibronectin in SaOS-2 cells on titanium surfaces: **a)** smooth (S); **b)** sandblasted-acid-etched (SBA); **c)** quantitative analysis: S vs SBA p=n.s. (not significant);

B) Western blotting expression of tenascin in SaOS-2 cells on titanium surfaces: **a)** smooth (S); **b)** sandblasted-acid-etched (SBA); **c)** quantitative analysis: S vs SBA p=n.s. (not significant).

Figure 6. Expression of type I collagen mRNA, in SaOS-2 cells cultured on smooth (S) or sandblasted-acid-etched (SBA) titanium surfaces, as shown by RT-PCR (panel A) and Real-time PCR (panel B): SBA vs S $p<0.05$.

Figure 7. Flow cytometric analysis of integrin expression of SaOS-2 cells cultured for 96 hrs on smooth (S) or sandblasted-acid-etched (SBA): SBA vs S $p<0.05$ for $\alpha 2$ subunits (panels A and B).

REFERENCES

1. ALBREKTSSON T, WENNERBERG A. Oral implant surfaces: Part 1-review focusing on topographic and chemical properties of different surfaces and in vivo responses to them. *Int J Prosthodont* 2004; **17:** 536-43.

2. ALBREKTSSON T, WENNERBERG A. Oral implant surfaces: Part 2-review focusing on clinical knowledge of different surfaces. *Int J Prosthodont* 2004; **17:** 544-64.

3. ALBREKTSSON T, BRANEMARK PI, HANSSON H, KASEMO B, LARSSON K, LUNDSTROM I, MCQUEEN DH, SKALAK R. The interface zone of inorganic implants in vivo: titanium implants in bone. *Ann Biomed Eng* 1983; **11:** 1-27.

4. ALBREKTSSON T, JOHANSSON C. Quantified bone tissue reactions to various metallic materials with reference to the so-called osteointegration concept. In: DAVIES JE, ed. *The bone-biomaterial interface*. Toronto: University of Toronto press; 1991: 357-63.

5. MASUDA T, YLIHEIKKILA PK, FELTON DA, COOPER LF. Generalizations regarding the process and phenomenon of osseointegration. Part I. In vivo studies. *Int J Oral Maxillofac Implants* 1998; **13:** 17-29.

6. COOPER LF, MASUDA T, YLIHEIKKILA PK, FELTON DA. Generalizations regarding the process and phenomenon of osseointegration. Part II. In vitro studies. *Int J Oral Maxillofac Implants* 1998; **13:** 163-74 .

7. MARTIN JY, SCHWARTZ Z, HUMMERT TW, SCHRAUB DM, SIMPSON J, LANKFORD J JR, DEAN DD, COCHRAN DL, BOYAN BD. Effect of titanium surface roughness on proliferation, differentiation, and protein synthesis of human osteoblast-like cells (MG63). *J Biomed Mater Res* 1995; **29:** 389-401.

8. WONG M, EULENBERGER J, SCHENK R, HUNZIKER E. Effect of surface topology on the osseointegration of implant materials in trabecular bone. *J Biomed Mater Res* 1995; **29:** 1567-75.

9. COCHRAN DL. Implant therapy I. *Ann Periodontol* 1996; **1:** 707-91.

10. COCHRAN DL. Endosseous dental implant surfaces in human clinical trials. A comparison using meta-analysis. *J Periodontol* 1999; **70:** 1523-39.

11. WIELAND M, SITTIG C, BRUNETTE DM, TEXTOR M, SPENCER ND. Measurement and evaluation of the chemical composition and topography of titanium implant surfaces. In: DAVIES JE, ed. *Bone Engineering*. Toronto: em squared Inc; 2000: 163-182.

12. THOMAS KA, COOK SD. An evaluation of variables influencing implant fixation by direct bone apposition. *J Biomed Mar Res* 1985; **19:** 875-901.

13. BUSER D, SCHENK RK, STEINEMANN S, FIORELLINI JP, FOX CH, STICH H. Influence of surface characteristics on bone integration of titanium implants. A histomorphometric study in miniature pigs. *J Biomed Mater Res* 1991; **25:** 889-902.

14. BRUNETTE DM. The effects of implant surface topography on the behaviour of cells. *Int J Oral Maxillofac Implants* 1988; **3:** 231-46.

15. WILKE JH, CLAES L, STEINEMANN S. The influence of various titanium surfaces on the interface shear strength between implants and bone. In: HEIMKE G, SOLTESZ U, LEE AJC, eds. *Clinical implant materials: Advances in Biomaterials*, vol. 9. Amsterdam: Elsevier Science Publishers BV; 1990: 309-14.

16. BOYAN BD, BATZER R, KIESWETTER K, LIU Y, COCHRAN DL, SZMUCKLER-MONCLER S, DEAN DD, SCHWARTZ Z. Titanium surface roughness alter responsiveness of MG63 osteoblast-like cells to 1 alpha, 25-(OH)2D3. *J Biomed Mater Res* 1998; **39:** 77-85.

17. POSTIGLIONE L, DI DOMENICO G, RAMAGLIA L, DI LAURO AE, DI MEGLIO F, MONTAGNANI S. Different titanium surfaces modulate the bone phenotype of SaOS-2 osteoblast-like cells. *Eur J Histochem* 2004; **48:** 213-22.

18. POSTIGLIONE L, DI DOMENICO G, RAMAGLIA L, MONTAGNANI S, SALZANO S, DI MEGLIO F, SBORDONE L, VITALE M, ROSSI G. Behavior of SaOS-2 cells cultured on different titanium surfaces. *J Dent Res* 2003; **82:** 692-6.

19. BRUNETTE DM. The effect of surface topography on cell migration and adhesion. In: RATNER BD, ed. *Surface characterization of Biomaterials*. Amsterdam: Elsevier Science Publishers; 1988: 203-17.

20. KIESWETTER K, SCHWARTZ Z, HUMMERT TW, COCHRAN DL, SIMPSON J, DEAN DD, BOYAN BD. Surface roughness modulates the local production of growth factors and cytokines by osteoblast-like MG-63 cells. *J Biomed Mater Res* 1996; **32:** 55-63.

21. GRONOWICZ G, KRAUSE A, MC CARTHY MB, COWLES EA. Integrin mediated signalling of osteoblasts on implant materials. In: Davies JE, ed. *Bone Engineering*. Toronto: em squared Inc; 2000: 256-66.

22. CHEN Q, KINCH MS, LIN TH, BURRIDGE K, JULIANO RL. Integrin-mediated cell adhesion activates mitogen-activated protein kinases. *J Biol Chem* 1994; **269:** 26602-5.

23. GRONOWICZ G, MCCARTHY MB. Response of human osteoblasts to implant materials: integrin-mediated adhesion. *J Orthop Res* 1996; **14:** 878-87.

24. INGBER DE, DIKE L, HANSEN L, KARP S, LILEY H, MANIOTIS A, MCNAMEE H, MOONEY D, PLOPPER G, SIMS J, WANG N. Cellular tensegrity: exploring how mechanical changes in the cytoskeleton regulate cell growth, migration, and tissue pattern during morphogenesis. *Int Rev Cytol* 1994; **150:** 173-224.

25. CAMPBELL CE, VON RECUM AF. Microtopography and soft tissue response. *J Invest Surg* 1989; **2:** 51-74.

26. RODAN SB, IMAI Y, THIEDE MA, WESOLOWSKI G, THOMPSON D, BAR-SHAVIT Z, SHULL S, MANN K, RODAN GA. Characterization of a human osteosarcoma cell line (Saos-2) with osteoblastic properties. *Cancer Res* 1987; **47:** 4961-6.

27. POSTIGLIONE L, DOMENICO GD, MONTAGNANI S, SPIGNA GD, SALZANO S, CASTALDO C, RAMAGLIA L, SBORDONE L, ROSSI G. Granulocyte-macrophage colony-stimulating factor (GM-CSF) induces the osteoblastic differentiation of the human osteosarcoma cell line SaOS-2. *Calcif Tissue Int* 2003; **72:** 85-97.

28. MURRAY E, PROVVEDINI D, CURRAN D, CATHERWOOD B, SUSSMAN H, MANOLAGAS S. Characterization of a human osteoblastic osteosarcoma cell line (SAOS-2) with high bone alkaline phosphatase activity. *J Bone Miner Res* 1987; **2:** 231-8.

29. FARLEY JR, HALL SL, HERRING S, TARBAUX NM, MATSUYAMA T, WERGEDAL JE. Skeletal alkaline phosphatase specific activity is an index of the osteoblastic phenotype in subpopulations of the human osteosarcoma cell line SaOS-2. *Metabolism* 1991; **40:** 664-71.

30. SHAPIRA L, HALABI A. Behavior of two osteoblast-like cell lines cultured on machined or rough titanium surfaces. *Clin Oral Impl Res* 2009; **20:** 50–55.

31. SANDBERG M, AUTIO-HARMAINEN H, VUORIO E. Localization of the expression of types I, III, and IV collagen, TGF-beta 1 and c-fos genes in developing human calvarial bones. *Dev Biol* 1988; **130:** 324-34.

32. NOMURA S, WILLS AJ, EDWARDS DR, HEATH JK, HOGAN BL. Developmental expression of 2ar (osteopontin) and SPARC (osteonectin) RNA as revealed by in situ hybridization. *J Cell Biol* 1988; **106:** 441-50.

33. WEINREB M, SHINAR D, RODAN GA. Different pattern of alkaline phosphatase, osteopontin, and osteocalcin expression in developing rat bone visualized by in situ hybridization. *J Bone Miner Res* 1990; **5:** 831-42.

34. ARONOW MA, GERSTENFELD LC, OWEN TA, TASSINARI MS, STEIN GS, LIAN JB. Factors that promote progressive development of the osteoblast phenotype in cultured fetal rat calvaria cells. *J Cell Physiol* 1990; **143:** 213-21.

35. OWEN TA, ARONOW M, SHALHOUB V, BARONE LM, WILMING L, TASSINARI MS, KENNEDY MB, POCKWINSE S, LIAN JB, STEIN GS. Progressive development of the rat osteoblast phenotype in vitro: reciprocal relationships in expression of genes associated with osteoblast proliferation and differentiation during formation of the bone extracellular matrix. *J Cell Physiol* 1990; **143:** 420-30.

36. POCKWINSE SM, WILMING LG, CONLON DM, STEIN GS, LIAN JB. Expression of cell growth and bone specific genes at single cell resolution during development of bone tissue-like organization in primary osteoblast cultures. *J Cell Biochem* 1992; **49:** 310-23.

37. STANFORD CM, KELLER JC. The concept of osseointegration and bone matrix expression. *Crit Rev Oral Biol Med* 1991; **2:** 83-101.

38. OSBORN JF, NEWESLEY H. Dynamics aspects of the implant-bone interface. In: HEIMKE G, ed. *Dental Implants Materials and Systems*. Munich: Carl Hanser; 1980: 111-123.

39. DAVIES JE. Mechanisms of endosseous integration. *Int J Prosthodont* 1998; **11:** 391-401.

40. DAVIES JE. Understanding peri-implant endosseous healing. *J Dent Educ* 2003; **67:** 932-49.

41. SCHWARTZ Z, LOHMANN CH, OEFINGER J, BONEWALD LF, DEAN DD, BOYAN BD. Implant surface characteristics modulate differentiation behavior of cells in the osteoblastic lineage. *Adv Dent Res* 1999; **13:** 38-48

42. DEGASNE I, BASLÉ MF, DEMAIS V, HURÉ G, LESOURD M, GROLLEAU B, MERCIER L, CHAPPARD D. Effects of roughness, fibronectin and vitronectin on attachment, spreading, and proliferation of human osteoblast-like cells (SaOS-2) on titanium surfaces. *Calcif Tissue Int* 1999; **64:** 499-507.

43. COOPER LF. A role for surface topography in creating and maintaining bone at titanium endosseous implants. *J Prosthet Dent* 2000; **84:** 522-34.

44. RAMAGLIA L, DI DOMENICO G, POSTIGLIONE L, MONTAGNANI S, ROSSI G, SBORDONE L. Proliferation and differentiation of human osteoblast-like cells on titanium surfaces. *J Dent Res* 2001; **80:** 213.

45. PARK JY, DAVIES JE. Red blood cell and platelet interactions with titanium implant surfaces. *Clin Oral Impl Res* 2000; **11:** 530-39.

46. SCHNEIDER G, BURRIDGE K. Formation of focal adhesion by osteoblast adhering to different substrata. *Exp Cell Res* 1994; **214:** 264-69.

47. CHOU L, FIRTH J, UITTO V, BRUNETTE D. Substratum surface topography alters cell shape and regulates fibronectin mRNA level, mRNA stability, secretion and assembly in human fibroblasts. *J Cell Sci* 1995; **108:** 1563-73.

48. BRUNETTE DM. Fibroblasts on micromachined substrata orient hierarchically to grooves of different dimensions. *Exp Cell Res* 1986; **164:** 11-26.

49. ZINGER O, ZHAO G, SCHWARTZ Z, SIMPSON J, WIELAND M, LANDOLT D, BOYAN B. Differential regulation of osteoblasts by substrate microstructural features. *Biomaterials* 2005; **26:** 1837-47.

50. SINHA RK, MORRIS F, SHAH SA, TUAN RS. Surface composition of orthopaedic implant metals regulates cell attachment, spreading, and cytoskeletal organization of primary human osteoblasts in vitro. *Clin Orthop Relat Res* 1994; **305:** 258–272.

51. YLIHEIKKILA PK, FELTON DA, WHITSON SW, AMBROSE WW, UOSHIMA K, COOPER LF. Correlative microscopic investigation of the interface between titanium alloy and the osteoblast–osteoblast matrix using mineralizing cultures of primary fetal bovinemandibular osteoblasts. *Int J Oral Maxillofac Implants* 1995; **10:** 655–665.

52. EL-GHANNAM A, DUCHEYNE P, SHAPIRO IM. Formation of surface reaction products on bioactive glass and their effects on the expression of the osteoblastic phenotype and the deposition of mineralized extracellularmatrix. *Biomaterials* 1997; **18:** 295–303.

53. SCHEVEN BA, MARSHALL D, ASPDEN RM. In vitro behaviour of human osteoblasts on dentin and bone. *Cell Biology International* 2002; **26:** 337–346.

54. ZHANG H, AHMAD M, GRONOWICZ G. Effects of transforming growth factor-beta 1 (tgfbeta1) on in vitro mineralization of human osteoblasts on implant materials. *Biomaterials* 2003; **24:** 2013–2020.

55. BACHLE M, KOHAL RJ. A systematic review of the influence of different titanium surfaces on proliferation, differentiation and protein synthesis of osteoblast-like mg63 cells. *Clin Oral Implants Res* 2004; **15:** 683–692.

56. LIAN JB, STEIN GS. The developmental stages of osteoblast growth and differentiation exhibit selective responses of genes to growth factors (TGF beta 1) and hormones (vitamin D and glucocorticoids). *J Oral Implantol* 1993; **19:** 95-105.

57. WOLFE SL. An introduction to cell and molecular biology. Belmont: Wadsworth Publishing Company; 1995.

58. HYNES RO, YAMADA KM. Fibronectins: multifunctional modular glycoproteins. *J Cell Biol* 1982; **95:** 369-77.

59. STEFFENSEN B, DUONG AH, MILAM SB, POTEMPA CL, WINBORN WB, MAGNUSON VL, CHEN D, ZARDENETA G, KLEBE RJ. Immunohistological localization of cell adhesion proteins and integrins in the periodontium. *J Periodontol* 1992; **63:** 584-92.

60. JONES FS, JONES PL. The Tenascin Family of ECM Glycoproteins: Structure, Function, and Regulation During Embryonic Development and Tissue Remodeling. *Dev Dyn* 2000; **218:** 235-259.

61. LOWENBERG BF, PILLIAR RM, AUBIN JE, FERNIE GR, MELCHER AH. Migration, attachment, and orientation of human gingival fibroblasts to root slices, naked and porous-surfaced titanium alloy discs, and Zircalloy 2 discs in vitro. *J Dent Res* 1987; **66:** 1000-5.